

## Exploring the Bounds on the Young's Modulus and Gravimetric Young's Modulus

Enlai Gao<sup>1,‡</sup>, Xiaoang Yuan,<sup>1</sup> Steven O. Nielsen<sup>2,†</sup>, and Ray H. Baughman<sup>1,2,3,\*</sup>

<sup>1</sup>*Department of Engineering Mechanics, School of Civil Engineering, Wuhan University, Wuhan, Hubei 430072, China*

<sup>2</sup>*Department of Chemistry and Biochemistry, The University of Texas at Dallas, Richardson, Texas 75080, USA*

<sup>3</sup>*Alan G. MacDiarmid NanoTech Institute, The University of Texas at Dallas, Richardson, Texas 75080, USA*



(Received 16 September 2021; revised 13 November 2021; accepted 24 May 2022; published 19 July 2022)

The continuous discovery of ultrahigh-modulus materials has increased the record for the Young's modulus and the gravimetric Young's modulus. However, the theoretical bounds on these moduli are still unknown. The upper bounds depend on the limits of the stiffness, alignment, and density of chemical bonds. From these limits, we here develop theoretical expressions for predicting the Young's modulus,  $Y_{\max} = [\hbar^2/(m_e^2 a_B^2)]\rho_e$ , and the gravimetric Young's modulus,  $Y_{\rho,\max} = [\hbar^2/(m_e m_p a_B^2)](N_e/A)$ , for ideal extreme-modulus solids, where  $\hbar$ ,  $m_e$ ,  $m_p$ ,  $a_B$ ,  $\rho_e$ , and  $N_e/A$  are the reduced Planck constant, electron mass, proton mass, Bohr radius, mass density of valence electrons, and the ratio of valence-electron number to atomic mass. By substituting the values of the nonconstant parameters ( $\rho_e$  and  $N_e/A$ ) for all elements into these expressions, the upper bounds on the Young's modulus and gravimetric Young's modulus are predicted to be 3074 GPa and 1036 GPa g<sup>-1</sup> cm<sup>3</sup>. These predictions are supported by the fact that the Young's modulus and gravimetric Young's modulus from a large set of experiments and first-principles calculations fall within these bounds. Moreover, by applying lateral pressure to linear carbyne crystals, the first-principles-calculated maximum Young's modulus and gravimetric Young's modulus are 2973 GPa and 968 GPa g<sup>-1</sup> cm<sup>3</sup>, respectively, which are near the predicted bounds. These carbyne crystals are predicted to have space group *R*-3*m*.

DOI: 10.1103/PhysRevApplied.18.014044

The Young's modulus ( $Y = \sigma/\varepsilon$ ) is a fundamental measure that quantifies the relationship between uniaxial stress ( $\sigma$ ) and strain ( $\varepsilon$ ). The closely related gravimetric Young's modulus ( $Y_\rho$ ), defined as the ratio of the Young's modulus to the mass density ( $\rho$ ), is also a fundamental metric, especially since lightweight materials with a high modulus are needed for numerous applications. We here predict the upper limits for the Young's modulus and gravimetric Young's modulus, and compare them with the moduli of materials observed or calculated in the highest-modulus direction. Since considerable work is required to identify, synthesize, and characterize extreme-modulus materials, we hope these results will guide such efforts towards theoretically realistic goals.

Diamond, having a Young's modulus of 1200 GPa, has long been known as the highest-modulus material, mainly because of its short stiff chemical bonds [1–3]. Considerable effort has been devoted to searching for ultrahigh-modulus materials (Fig. 1). In 1955 and 1957, diamond and cubic boron nitride ( $Y \approx 1000$  GPa)

were synthesized by the General Electric Company [4,5]. In 1966, osmium ( $Y \approx 560$  GPa) and iridium ( $Y \approx 538$  GPa) were found to exhibit the highest Young's moduli in the group of platinum metals [6]. In 2008, Lee *et al.* [7] measured a Young's modulus of approximately 1000 GPa for a graphene monolayer.

Using first-principles calculations and data-driven techniques, an increasing number of ultrahigh-modulus crystals have been computationally discovered. In 2011, Li *et al.* [8] predicted that lonsdaleite ( $Y = 1325$  GPa) was stiffer than diamond. More recently, the modulus limits were predicted for a fiber comprising nanotube-wrapped carbynes (NTWCs). The carbyne chains serve as reinforcing structures, and the carbon-nanotube sheath protects the multiple carbyne chains against reaction. The highest calculated Young's modulus and the gravimetric Young's modulus of NTWCs are determined to be 1505 GPa and 977 GPa g<sup>-1</sup> cm<sup>3</sup> [9]. In 2021, two ultrahigh-modulus crystals ( $\text{CN}_2$  and  $\text{OsN}_2$ ), with maximum Young's moduli of 1555 and 1383 GPa, respectively, were discovered by data-mining first-principles calculations for 13 122 crystals [10].

The discovery of ultrahigh-modulus materials has significantly increased the records for the Young's modulus and the gravimetric Young's modulus (Fig. 1). However,

\*ray.baughman@utdallas.edu

†steven.nielsen@utdallas.edu

‡enlaigao@whu.edu.cn

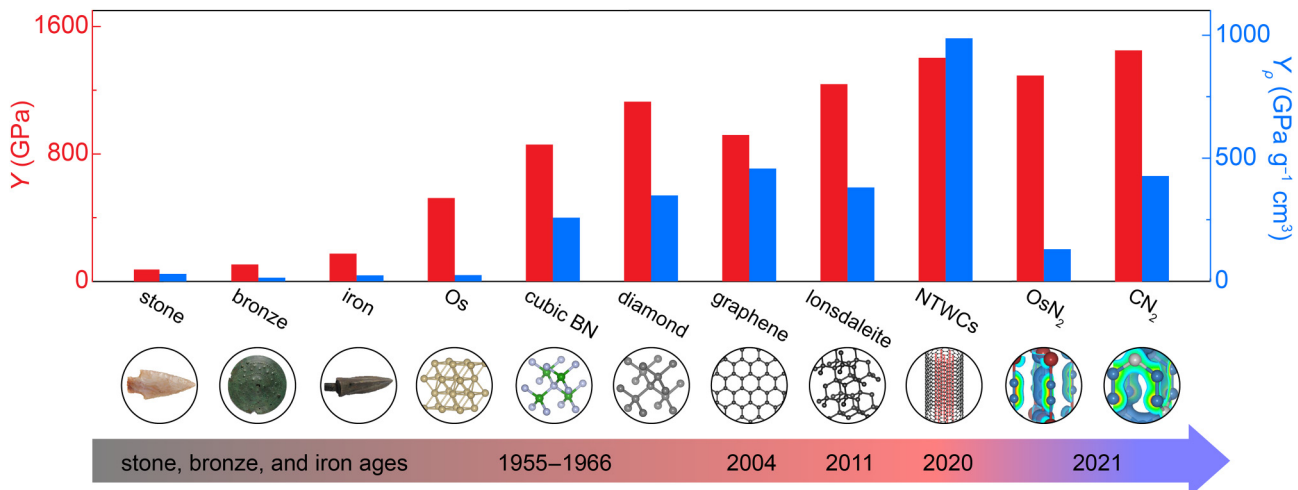


FIG. 1. Brief history of the Young's modulus (red bars) and gravimetric Young's modulus (blue bars) in the highest-modulus direction.

the theoretical upper bounds on these moduli are still unknown. The Young's modulus of known bulk materials never reaches several terapascal, which is mainly due to the upper limits of the stiffness, alignment, and density of chemical bonds. Bounds on and insights into such values would provide guidelines for finding ultrahigh-modulus materials. Hence, the present goal is to establish the bounds on the Young's modulus and gravimetric Young's modulus.

Since the Young's modulus is direction dependent, it is reasonable to imagine that the best candidate structure for obtaining an extreme modulus has the following features: all chemical bonds are stiff, aligned in the tensile direction, and densely packed. As the bond polarity of materials increases, the chemical bonds can vary from covalent to ionic bonds. Compared with ionic bonds, covalent bonds formed between atoms with similar electronegativity are generally shorter and stiffer. Hence, the known stiffest chemical bonds are covalent and the known highest-modulus solids are covalent solids. Our previous findings of the highest-modulus materials and the modulus-structure correlation support this expectation [9,10]. Herein, we assume that an ideal extreme-modulus solid consists of linear covalent bonds (Fig. 2). Under these conditions, the relationship between the Young's modulus,  $Y$ , and the bond-force constant,  $k$ , is

$$Y = \frac{kr}{s} = \frac{kr^2}{V_a}, \quad (1)$$

where  $s$  and  $r$  are the cross-section area per chain and the bond length, respectively, and  $V_a = sr$  is the atomic volume (volume per atom). It is found that the force constant is inversely proportional to the square of the equilibrium internuclear distance for the known stiffest chemical

bonds [11], that is,  $kr^2 = fE_R$ , where  $f$  is a prefactor and  $E_R$  is the Rydberg energy constant. With the reduced Planck constant, the electron mass, and the Bohr radius, denoted by  $\hbar$ ,  $m_e$ , and  $a_B$ , respectively, the Rydberg energy constant can be expressed as  $E_R = \hbar^2/(2m_e a_B^2)$ . The known stiffest chemical bonds are within diatomic molecules consisting of the elements in Group IVA ( $C_2$ ,  $Si_2$ ) and Group VA ( $N_2$ , etc.), in which  $kr^2$  are about  $8E_R$  and  $10E_R$ , respectively [11]. These data indicate that  $f$  is approximately  $2N_e$ , where  $N_e$  is the number of valence electrons of the element, and thus,  $kr^2 = 2N_e E_R$  for these known stiffest bonds. Hence, the Young's modulus for ideal extreme-modulus solids consisting of these bonds can be written as

$$Y_{\max} = \left( \frac{\hbar}{m_e a_B} \right)^2 \frac{N_e m_e}{V_a}. \quad (2)$$

Furthermore, the mass density of the valence electrons ( $\rho_e$ ) can be defined as

$$\rho_e = \frac{N_e m_e}{V_a}. \quad (3)$$

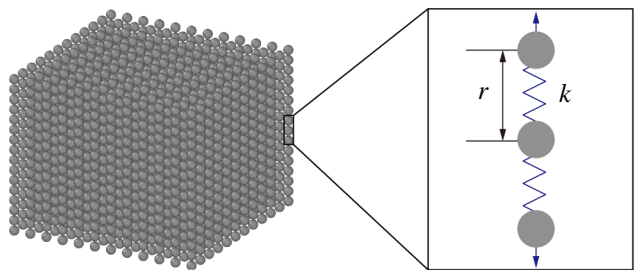


FIG. 2. Illustration of ideal extreme-high-modulus solids, in which all chemical bonds are stiff, aligned in the tensile direction, and densely packed.

Thus,  $Y_{\max}$  and  $\rho_e$  are related as

$$Y_{\max} = \left( \frac{\hbar}{m_e a_B} \right)^2 \rho_e. \quad (4)$$

The Young's modulus of any realistic material should be lower than this ideal case, that is,  $Y \leq Y_{\max}$ .

Meanwhile, the gravimetric Young's modulus for ideal extreme-modulus solids can be derived as

$$Y_{\rho,\max} = \left( \frac{\hbar}{m_e a_B} \right)^2 \frac{\rho_e}{\rho}, \quad (5)$$

where  $\rho$  is the mass density of the solid that can be written as

$$\rho = \frac{Am_p}{V_a}, \quad (6)$$

where  $A$  is the unitless atomic mass (i.e., the atomic mass divided by the proton mass) and  $m_p$  is the proton mass. Therefore,  $Y_{\rho,\max}$  can be derived as

$$Y_{\rho,\max} = \frac{\hbar^2}{m_e m_p a_B^2} (N_e/A). \quad (7)$$

Equations (4) and (7) indicate that  $Y_{\max}$  depends only on  $\rho_e$  and  $Y_{\rho,\max}$  solely depends on  $N_e/A$ , since all other parameters in these expressions are fundamental physical constants. Hence, the upper bounds on the Young's modulus and gravimetric Young's modulus can be obtained by searching for the maximum values of  $\rho_e$  and  $N_e/A$ , respectively. To this end, we examine  $\rho_e$  and  $N_e/A$  for the elements. For each element,  $\rho_e$  is calculated from  $N_e$  and  $V_a$ , and  $N_e/A$  is calculated from  $N_e$  and  $A$ . Notably,  $V_a$  for each element is from the known densest phase of this element [12]. Figure 3 shows that the highest value of  $\rho_e$  is obtained for carbon, while the highest value of  $N_e/A$  is obtained for neon. Substituting these highest values into Eqs. (4) and (7), the upper bounds on the Young's modulus and gravimetric Young's modulus are obtained as

$$Y_{\max} = \frac{4\hbar^2}{m_e a_B^2 V_{\text{carbon}}} = 3074 \text{ GPa}, \quad (8)$$

and

$$Y_{\rho,\max} = \frac{8\hbar^2}{m_e m_p a_B^2 A_{\text{neon}}} = 1036 \text{ GPa g}^{-1} \text{ cm}^3, \quad (9)$$

where  $V_{\text{carbon}}$  and  $A_{\text{neon}}$  are the atomic volume of carbon ( $5.68 \text{ \AA}^3$ ) and the unitless atomic mass of neon (20.18), respectively. These bounds should be treated as estimates, since their accuracies are determined by atomic values and model assumptions. Interestingly, even if neon is omitted,

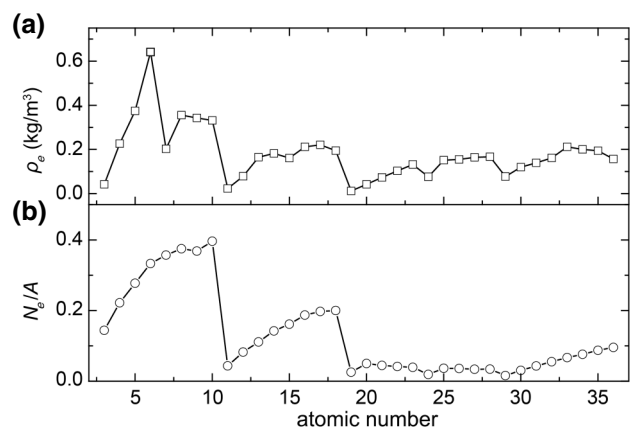


FIG. 3. (a) Mass density of valence electrons ( $\rho_e$ ), and (b) ratio of the number of valence electrons to the atomic mass ( $N_e/A$ ) for different elemental solids.

which is unlikely to form linear-chain covalent solids with any elements,  $Y_{\rho,\max}$  is only lowered by 7%, 5%, 10%, and 16%, when the parameters for fluorine, oxygen, nitrogen, or carbon, respectively, are used [Fig. 3(b)]. It should be noted that the atomic volume is one of the most important parameters, so we confirm the reliability of these data by comparison with two more recent databases (see the Supplemental Material for details [13,14]). In comparison with prior studies, the magnitudes of the bulk and shear moduli for isotropic solids can be quickly estimated through dimensional analysis [15]. However, this estimation is rough: for example, the estimated bulk modulus for Na is about 3 times the experimental value [15]. Hence, such dimensional analysis cannot be used for determining the upper bound for either the bulk modulus or the Young's modulus.

To provide support for the predicted bounds on the Young's modulus and the gravimetric Young's modulus, we compare these predictions with previously reported results. The moduli of high-modulus materials from a literature survey are summarized in Table S1 within the Supplemental Material [1,8–10,13,16–21]. Considering controversies in the cross-section area and the Young's modulus for low-dimensional materials [9,22], only the noncontroversial gravimetric Young's modulus for such materials is discussed. The highest Young's modulus and gravimetric Young's modulus are found for  $\text{CN}_2$  (1555 GPa) and NTWC (977 GPa  $\text{g}^{-1} \text{ cm}^3$ ), respectively. These extreme values fall within the predicted upper bounds on the Young's modulus (3074 GPa) and gravimetric Young's modulus (1036 GPa  $\text{g}^{-1} \text{ cm}^3$ ), respectively (Fig. 4).

Furthermore, we compare these predictions with database results for a large set of materials. Figure 4 shows the distribution of the maximum Young's modulus and maximum gravimetric Young's modulus obtained from

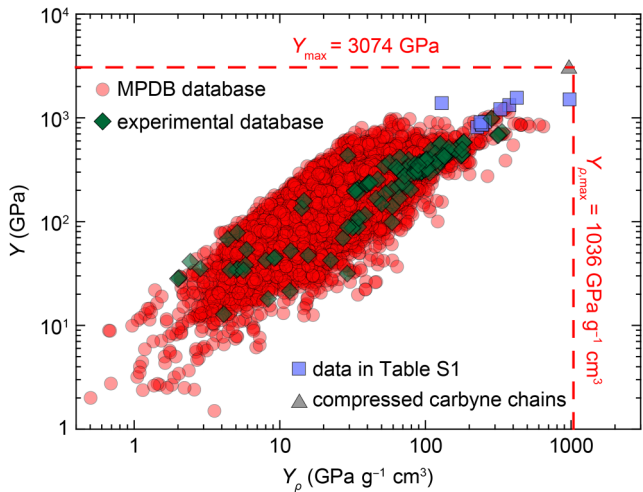


FIG. 4. Predicted bounds on the Young’s modulus and gravimetric Young’s modulus (dotted red lines), compared with the Young’s modulus and gravimetric Young’s modulus calculated from the MPDB [23], the database of experimental elastic tensors [24], data in Table S1 within the Supplemental Material [1,8–10,13,16–21], and our calculated data for compressed carbyne chains.

DFT-calculated elastic tensors for 11 401 materials and experimental elastic tensors for 136 materials. These tensors are from the materials project database (MPDB [23]) of elastic tensors from first-principles calculations [23] and the database of experimental elastic tensors [24]. These results show that the Young’s modulus and the gravimetric Young’s modulus from both calculations and experiments fall within their predicted bounds.

Figure 4 shows that the highest gravimetric Young’s modulus (NTWC, 977  $\text{GPa g}^{-1} \text{cm}^3$ ) approaches the predicted upper bound ( $1036 \text{ GPa g}^{-1} \text{cm}^3$ ), while the highest Young’s modulus ( $\text{CN}_2$ , 1555 GPa) is only about half of the predicted upper bound (3074 GPa). These results suggest that there is plenty of room for increasing the Young’s modulus to the predicted bound. Considering that the proposed extreme-modulus materials have an extreme structure (all bonds are stiff, aligned in the tensile direction, and densely packed), we calculate the Young’s modulus for compressed carbyne chains, which are currently the leading candidate structure for obtaining the highest Young’s modulus. As detailed below, this choice provides a predicted Young’s modulus of 2973 GPa, which is very close to the upper bound of 3074 GPa (Fig. 4).

We previously predicted that confining a large array of carbyne chains within a carbon nanotube would result in a high-modulus material [9]. In such an arrangement, the carbyne chains act as stiffening structures, while the nanotube sheath acts as a confining and protective host. The axial Young’s modulus of this material is 1505 GPa, when restricted to assemblies with a positive binding energy [9].

To increase this value, Eqs. (2) and (4) indicate that we should decrease  $V_a$  or increase  $\rho_e$ . More specifically, if the nanotube sheath is filled with more carbyne chains, it is possible to increase the Young’s modulus by an interchain-pressure-induced decrease of  $V_a$  (or increase of  $\rho_e$ ).

To investigate the Young’s modulus for such confined carbyne chains, we perform density-functional-theory (DFT) calculations with the Vienna *ab initio* simulation package [25], using the Perdew-Burke-Ernzerhof parameterization [26] of the generalized gradient approximation and the projector-augmented wave basis set [27], with an energy cutoff of 520 eV. A 75-*k*-point mesh along the chain is used for Brillouin zone sampling [28]. The conjugate-gradient algorithm is used for structural relaxation, until the force on each atom converges to below 0.001 eV/Å. To decrease the computational cost of the DFT calculations, we omit the nanotube sheath and produce such interchain pressure by fixing the transverse size of the carbyne crystal. Unit cells of the energy-minimized carbyne crystals with different interchain spacings ( $d$ ) are constructed [Fig. 5(a)]. The atomic and electronic structures of the laterally compressed carbyne chains are shown in Fig. 5(b). The axial Young’s moduli of these structures are calculated by applying a tensile strain of 1%. Figure 5(c) shows that the Young’s modulus first increases and then decreases with decreasing  $V_a$  (corresponding to increasing  $\rho_e$ ). The Young’s modulus for carbyne crystals increases from 1271 GPa to a peak value of 2973 GPa, when the atomic volume per carbon is compressed from its equilibrium value of 15.2 to 5.4 Å<sup>3</sup>. This highest Young’s modulus is very close to the upper bound for any material of 3074 GPa [Fig. 4]. As the atomic volume further decreases, the Young’s modulus drops and deviates from Eqs. (2) and (4). The breakdown from the Eqs. (2) and (4) dependence is due to strong interchain repulsion, which forces the elongation and weakening of the bonds along the axial direction, from which the Young’s modulus is calculated [Fig. 5(b)].

Since the crystal and molecular structures of carbyne remain controversial, we here provide an additional theoretical evaluation. Even whether the chain is a polyyne ( $-\text{C}\equiv\text{C}-$ ) or a cumulene ( $=\text{C}=\text{C}=$ ) is uncertain, since the Yakobson group’s single-chain calculations reveal that the polyyne structure is more stable than the cumulene structure by only 2 meV per atom [29]. Considering the small energy difference between cumulene and polyyne, additional energy-convergence tests are performed and a stringent convergence criterion of the energy ( $10^{-5}$  eV/atom) is adopted to ensure accurate results (Fig. S3 within the Supplemental Material [13]). Our results for single chains also predict that the polyyne chain is slightly more stable than the cumulene chain. An important issue is whether interchain interactions can reverse this stability. Using empirical potentials and molecular-mechanics

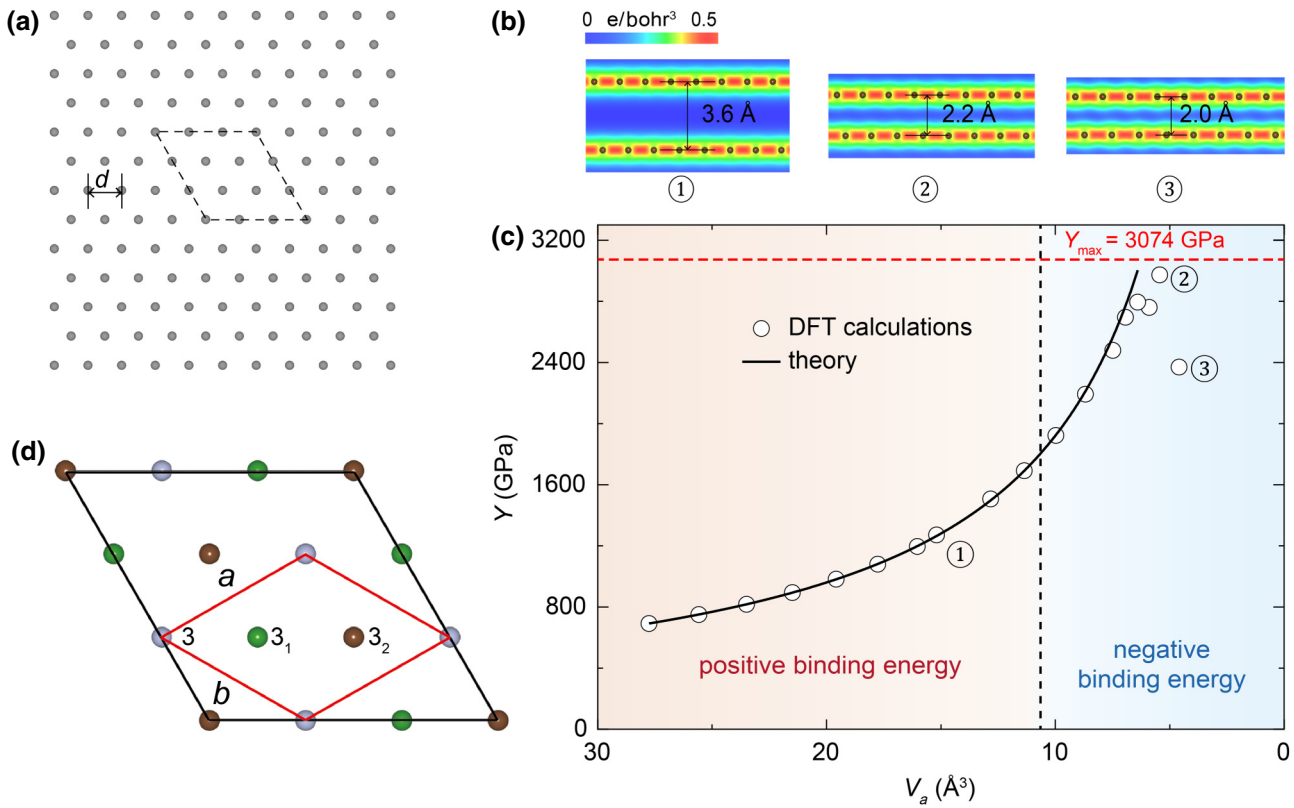


FIG. 5. (a) Top and side views of the carbyne crystal structure. Computational cell is denoted by the dashed box. (b) Atomic and electronic structures of compressed carbyne chains. (c) Young's modulus ( $Y$ ) for compressed carbyne crystals as a function of atomic volume ( $V_a$ ). Binding energy is defined as the sum of the energy of noninteracting carbyne chains minus the total energy of compressed carbyne chains (normalized per atom). (d) Predicted crystal structure that minimizes the total energy for both cumulene and polyyne chain crystals, in which the primitive cell is denoted by the red box. In this structure, there are three types of carbon chains, which have axial symmetries of 3 (gray chains), 3<sub>1</sub> (green chains), and 3<sub>2</sub> (brown chains), where the 3<sub>1</sub> and 3<sub>2</sub> chains are related by mirror planes. Predicted equilibrium unit-cell parameters are  $a = b = 6.409 \text{ \AA}$  and  $c = 1.281 \text{ \AA}$  for the cumulene crystal and  $a = b = 6.436 \text{ \AA}$  and  $c = 2.565 \text{ \AA}$  for the polyyne crystal. Atomic fractional coordinates for the primitive cells are (0,0,0) for the cumulene crystal and (0,0,0.2546) for the polyyne crystal.

calculations, Belenkoy and Mavrinsky [30] found that a cumulene crystal was more stable than a polyyne crystal by 0.2 meV per atom. Since these energy differences are so small, we reevaluate the energetically-most-stable crystal phases for both polyyne and cumulene chains. In both cases, we find that the most stable crystal phase has a trigonal structure with space group  $R\bar{3}m$  [Fig. 5(d)]. While our results also predict that the cumulene crystal has a lower energy than the polyyne crystal, this space group ( $R\bar{3}m$ ) has not previously been predicted to minimize the total energy for either chain type. Nevertheless, Raman data for both carbyne crystals [31] and carbyne chains [32] confined within carbon nanotubes indicate the presence of triple bonds.

Some additional remarks follow. First, the modulus bounds provide useful estimates for the tensile strength of defect-free solids. For an ideal solid, Frenkel's model indicates that the intrinsic strength is about 1/10 of the Young's modulus [33]. This is generally consistent with more recent

results, which predict that defect-free crystals would break at a stress of  $Y/8$ – $Y/15$  [34–36]. Based on this upper limit and the above-determined upper bounds on the Young's modulus and gravimetric Young's modulus, the upper bounds on the theoretical strength and gravimetric strength can be roughly estimated as 384 GPa and 130 GPa g<sup>-1</sup> cm<sup>3</sup>. A literature survey shows that the highest calculated strength and gravimetric strength for any material are 225 GPa and 92 GPa g<sup>-1</sup> cm<sup>3</sup> for diamond and linear BC chains, respectively [1,37]. Our calculations on the tensile strength of laterally confined carbyne chains demonstrate that the maximum strength and gravimetric strength are 251 GPa and 105 GPa g<sup>-1</sup> cm<sup>3</sup>. Hence, the known highest strength and highest gravimetric strength are below, but approaching, the presently estimated upper bounds.

Second, the modulus bounds provide useful estimates for the upper limit of the sound speed. The sound speed for solids can be written as  $V = \sqrt{Y(1-\nu)/\rho(1+\nu)(1-2\nu)}$ , where  $\nu$  is the Poisson's ratio. By adopting a typical

Poisson's ratio of 0.3, the upper limit of the speed of sound can be roughly estimated as 37 km/s from the bound on the gravimetric modulus ( $Y_{\rho,\max} = 1036 \text{ GPa g}^{-1} \text{ cm}^3$ ). This estimate is very close to the upper limit of the speed of sound (36 km/s) predicted by Trachenko *et al.* [38].

Third, we find that the bounds on the moduli are different for different crystal structures. Equation (7) is derived for ideal extreme-modulus materials. By introducing a loss factor,  $f$ , this equation can be generalized for predicting the gravimetric Young's modulus for crystal structures in which the chemical bonds might not be stiff or uniformly aligned, i.e.,  $Y_\rho = f Y_{\rho,\max}$ . The physical meaning of the loss factor is the deviation of chemical-bond stiffnesses and crystal structures from those of ideal extreme-modulus materials. Based on this equation,  $f$  can be calculated as 0.33, 0.44, and 0.93 for diamond, graphene, and carbyne structures, respectively, mainly determined by the stiffness and alignment of bonds along the highest-modulus direction. The loss-factor ratio of cubic diamond and graphene to carbyne are 0.36 and 0.47, respectively, and the loss-factor ratio of cubic BN and *h*-BN to linear BN chains are 0.31 and 0.41, respectively. These results suggest that the moduli are largely determined by bonding dimensionality.

In summary, we derive theoretical expressions for predicting the Young's modulus,  $Y_{\max} = [\hbar^2/(m_e^2 a_B^2)] \rho_e$ , and gravimetric Young's modulus,  $Y_{\rho,\max} = [\hbar^2/(m_e m_p a_B^2)] (N_e/A)$ , for ideal extreme-modulus solids from the limits of the stiffness, alignment, and density of chemical bonds. The upper bounds on the Young's modulus and gravimetric Young's modulus are determined to be 3074 GPa and  $1036 \text{ GPa g}^{-1} \text{ cm}^3$ , respectively. Our predictions are supported by the fact that the Young's modulus and gravimetric Young's modulus from a large set of experiments and first-principles calculations fall within the predicted bounds. Finally, we laterally compress carbyne crystals to above their stability limit and show that the calculated highest Young's modulus (2973 GPa) and gravimetric Young's modulus ( $968 \text{ GPa g}^{-1} \text{ cm}^3$ ) approach the predicted bounds. These carbyne crystals have the predicted space group *R*-3*m*.

## ACKNOWLEDGMENTS

This work in China is supported by the National Natural Science Foundation of China (Grant No. 12172261). This work in the USA is supported by the Robert A. Welch Foundation Grant No. AT-0029. The numerical calculations in this work are done on the supercomputing system in the Supercomputing Center of Wuhan University.

[1] R. H. Telling, C. J. Pickard, M. C. Payne, and J. E. Field, Theoretical Strength and Cleavage of Diamond, *Phys. Rev. Lett.* **84**, 5160 (2000).

- [2] C. Dang, J. P. Chou, B. Dai, C. T. Chou, Y. Yang, R. Fan, W. Lin, F. Meng, A. Hu, J. Zhu, *et al.*, Achieving large uniform tensile elasticity in microfabricated diamond, *Science* **371**, 76 (2021).
- [3] Y. Zhang, H. Sun, and C. Chen, Atomistic Deformation Modes in Strong Covalent Solids, *Phys. Rev. Lett.* **94**, 145505 (2005).
- [4] F. P. Bundy, H. T. Hall, H. M. Strong, and R. H. Wentorfjun, Man-made diamonds, *Nature* **176**, 51 (1955).
- [5] R. H. Wentorf, Cubic form of boron nitride, *J. Chem. Phys.* **26**, 956 (1957).
- [6] A. Darling, The elastic and plastic properties of the platinum metals, *Platinum Met. Rev.* **10**, 14 (1966).
- [7] C. Lee, X. Wei, J. W. Kysar, and J. Hone, Measurement of the elastic properties and intrinsic strength of monolayer graphene, *Science* **321**, 385 (2008).
- [8] Q. Li, Y. Sun, Z. Li, and Y. Zhou, Lonsdaleite – a material stronger and stiffer than diamond, *Scr. Mater.* **65**, 229 (2011).
- [9] E. Gao, R. Li, and R. H. Baughman, Predicted confinement-enhanced stability and extraordinary mechanical properties for carbon nanotube wrapped chains of linear carbon, *ACS Nano* **14**, 17071 (2020).
- [10] Q. Shao, R. S. Li, Z. G. Yue, Y. L. Wang, and E. L. Gao, Data-driven discovery and understanding of ultrahigh-modulus crystals, *Chem. Mater.* **33**, 1276 (2021).
- [11] R. P. Smith, The relationship of force constant and bond length, *J. Phys. Chem.* **60**, 1293 (2002).
- [12] C. N. Singman, Atomic volume and allotropy of the elements, *J. Chem. Educ.* **61**, 137 (1984).
- [13] See the Supplemental Material at <http://link.aps.org/supplemental/10.1103/PhysRevApplied.18.014044> for details of the comparison of atomic volume data with more recent databases, energy-convergence tests of DFT calculations on cumulene and polyyne, and the Young's modulus and gravimetric Young's modulus in the highest-modulus direction for typical high-modulus materials from a literature survey, which includes Refs. [1,8–10,12,14,16–21].
- [14] R. Hoffmann, A. A. Kabanov, A. A. Golov, and D. M. Proserpio, *Homo citans* and carbon allotropes: For an ethics of citation, *Angew. Chem., Int. Ed. Engl.* **55**, 10962 (2016).
- [15] E. N. Economou, *The Physics of Solids: Essentials and Beyond* (Springer, New York, 2010), p. 34.
- [16] B. Kulnitskiy, I. Perezhigin, G. Dubitsky, and V. Blank, Polytypes and twins in the diamond-lonsdaleite system formed by high-pressure and high-temperature treatment of graphite, *Acta Crystallogr., Sect. B* **69**, 474 (2013).
- [17] X. Jiang, J. Zhao, and R. Ahuja, A novel superhard BN allotrope under cold compression of *h*-BN, *J. Phys.: Condens. Matter* **25**, 122204 (2013).
- [18] Q. Li, H. Liu, D. Zhou, W. Zheng, Z. Wu, and Y. Ma, A novel low compressible and superhard carbon nitride: Body-centered tetragonal CN<sub>2</sub>, *Phys. Chem. Chem. Phys.* **14**, 13081 (2012).
- [19] J. Wu, B. Wang, Y. Wei, R. Yang, and M. Dresselhaus, Mechanics and mechanically tunable band gap in single-layer hexagonal boron-nitride, *Mater. Res. Lett.* **1**, 200 (2013).
- [20] R. Wang, W. Pan, M. Jiang, J. Chen, and Y. Luo, Investigation of the physical and mechanical properties of

- hot-pressed machinable  $\text{Si}_3\text{N}_4/h$ -BN composites and FGM, *Mater. Sci. Eng., B* **90**, 261 (2002).
- [21] C. Cab, J. Medina, M. L. Casais-Molina, G. Canto, and A. Tapia, Ultrahigh stretching bond force constants of linear chains of carbon and boron nitride, *Carbon* **150**, 349 (2019).
- [22] E. Gao and Z. Xu, Thin-shell thickness of two-dimensional materials, *J. Appl. Mech.* **82**, 121012 (2015).
- [23] M. de Jong, W. Chen, T. Angsten, A. Jain, R. Notestine, A. Gamst, M. Sluiter, C. Krishna Ande, S. van der Zwaag, J. J. Plata, *et al.*, Charting the complete elastic properties of inorganic crystalline compounds, *Sci. Data* **2**, 150009 (2015).
- [24] Y. Zhang and J. Ma, *Handbook of Ceramic Materials* (Chemical Industry Press, Beijing, 2006).
- [25] G. Kresse and J. Furthmüller, Efficiency of *ab-initio* total energy calculations for metals and semiconductors using a plane-wave basis set, *Comput. Mater. Sci.* **6**, 15 (1996).
- [26] J. P. Perdew, K. Burke, and M. Ernzerhof, Generalized Gradient Approximation Made Simple, *Phys. Rev. Lett.* **77**, 3865 (1996).
- [27] P. E. Blöchl, Projector augmented-wave method, *Phys. Rev. B* **50**, 17953 (1994).
- [28] H. J. Monkhorst and J. D. Pack, Special points for Brillouin-zone integrations, *Phys. Rev. B* **13**, 5188 (1976).
- [29] M. Liu, V. I. Artyukhov, H. Lee, F. Xu, and B. I. Yakobson, Carbyne from first principles: Chain of C atoms, a nanorod or a nanorope, *ACS Nano* **7**, 10075 (2013).
- [30] E. A. Belenkova and V. V. Mavrin, Crystal structure of a perfect carbyne, *Crystallogr. Rep.* **53**, 83 (2008).
- [31] B. Pan, J. Xiao, J. Li, P. Liu, C. Wang, and G. Yang, Carbyne with finite length: The one-dimensional *sp* carbon, *Sci. Adv.* **1**, e1500857 (2015).
- [32] L. Shi, P. Rohringer, K. Suenaga, Y. Niimi, J. Kotakoski, J. C. Meyer, H. Peterlik, M. Wanko, S. Cahangirov, A. Rubio, *et al.*, Confined linear carbon chains as a route to bulk carbyne, *Nat. Mater.* **15**, 634 (2016).
- [33] J. Frenkel, Zur Theorie der Elastizitätsgrenze und der Festigkeit kristallinischer Körper, *Z. Phys.* **37**, 572 (1926).
- [34] M. F. Ashby, Overview no. 80: On the engineering properties of materials, *Acta Metall.* **37**, 1273 (1989).
- [35] B. I. Yakobson and P. Avouris, in *Carbon Nanotubes*, edited by M. S. Dresselhaus, G. Dresselhaus, P. Avouris (Springer, New York, 2001), p. 287.
- [36] R. C. Cooper, C. Lee, C. A. Marianetti, X. Wei, J. Hone, and J. W. Kysar, Nonlinear elastic behavior of two-dimensional molybdenum disulfide, *Phys. Rev. B* **87**, 035423 (2013).
- [37] E. Gao, Y. Guo, Z. Wang, S. O. Nielsen, and R. H. Baughman, The strongest and toughest predicted materials: Linear atomic chains without a Peierls instability, *Matter* **5**, 1192 (2022).
- [38] K. Trachenko, B. Monserrat, C. J. Pickard, and V. V. Brazhkin, Speed of sound from fundamental physical constants, *Sci. Adv.* **6**, eabc8662 (2020).